A 3D Vision Based Approach for Optimal Grasp of Vacuum Grippers

Angel J. Valencia[1], Roger M. Idrovo[1], Angel D. Sappa[1,2], Douglas Plaza Guingla[1], Daniel Ochoa[1]

[1] ESPOL Polytechnic University, Escuela Superior Politécnica del Litoral, ESPOL,
Facultad de Ingeniería en Electricidad y Computación,
Campus Gustavo Galindo Km 30.5 Vía Perimetral, P.O. Box 09-01-5863, Guayaquil, Ecuador

[2]Computer Vision Center, Edifici O, Campus UAB,
08193, Bellaterra, Barcelona, Spain

{ajvalenc, romiidro, asappa, douplaza, dochoa}@espol.edu.ec

***Abstract*—In general, robot grasping approaches are based on the usage of multi-finger grippers. However, when large size objects need to be manipulated vacuum grippers are preferred, instead of finger based grippers. This paper aims to estimate the best picking place for a two suction cups vacuum gripper, when planar objects with an unknown size and geometry are considered. The approach is based on the estimation of geometric properties of object's shape from a partial cloud of points (a single 3D view), in such a way that combine with considerations of a theoretical model to generate an optimal contact point that minimizes the vacuum force needed to guarantee a grasp. Experimental results in real scenarios are presented to show the validity of the proposed approach.**

I. Introduction

Efficient grasping is an essential requirement in any manipulation task. It is intended to guarantee a firm grasp with the minimum energy. This requirement becomes a real drawback in those cases where the robot needs to pick up unknown objects, which can be of different geometries and sizes. In order to tackle this problem, several approaches have been proposed in the literature [1]. In that context, computer vision has actively contributed in object perception to extract characteristics that help to estimate the efficient grasp; this integration is mandatory in current robotics applications. Most of the approaches mentioned above relies on the usage of grippers or finger like grasping. On the contrary, efficient passive based grasping approaches (i.e., holding objects without gripper or fingers) have been slightly studied in the literature.

During last decades computer vision has become an ubiquitous technology that allows to easily interact with objects in unstructured environments. We can find vision based approaches in different applications, from 3D measurement [2] or industrial applications (e.g., [3], [4]) till scene modeling [5] or driving assistance [6], just to mention a few. Coarsely speaking computer vision based approaches can be classified in monocular or 3D; monocular approaches rely on a projection of the scene into a 2D representation (2D images), while 3D based approaches use 3D information of the scene (3D images) obtained from depth cameras (e.g., structured light systems [2], stereovision [4]). In the context of grasping, 3D based approaches are preferred since objects and scene geometry can be captured.

Briefly speaking, with depth cameras cloud of points are obtained to produce an object representation and thus generate a grasp planner according to the estimated contact point. One of the problems in this step is to obtain a good model of the object using just a single view, which give a partial cloud of points of the object. In most of the cases it comes from a single depth image and become a challenge to define a suitable grasp due to the possibility that the contact point lay in the missing parts. As a result of this, many approaches are interested in obtaining a model as faithful as possible to the original one. However, generating a complete shape description is in general a time consuming task and in some cases it is not necessary to know in order to generate a valid grasp.

As mentioned above, another relevant factor in the grasping process is the kind of gripper utilized. Passive grippers, and in particular vacuum grippers, require a flat surface to place their cups. This characteristic makes them suitable to manage large size planar objects. So far, different methods in grasp optimization implement an analysis of gripper-object based on a force-closure approach, but since vacuum grippers have a different working principle, another set of parameters, such as vacuum force and suction cups localization, should be consider.

In this paper we present a system that improves grasping of unknown objects for robot manipulators equipped with vacuum grippers. The proposed approach is based on the estimation of geometric properties from the object's partial shape using a single depth image, similar to the work proposed by [7]. Since we are focused in vacuum grippers, only objects with flat surfaces are considered. These properties are later on used by a theoretical model based on force and moment equilibrium equations of gripper-object, which was introduced by Mantriota in [8]. Based on this study, we define the minimum contact pressure and the most suitable position of the vacuum gripper that guarantee a reliable grasp.

The rest of the paper is organized as follows. Section II briefly summarizes relevant literature. Section III describes the

methods used in the proposed grasping optimization system. Section IV presents a series of experiments to evaluate the proposed approach. Finally, in Section V, conclusions and future works are summarized.

II. Related Work

Recent works in grasping objects with unknown geometry consider handling a partial view of them, obtained by a cloud of 3D points. Gallardo et al. have proposed to fit a set of shape primitives (e.g., boxes and cylinders) to describe the object's overall shape, as well as its location, orientation and size [9]. Similarly, the works of Rodriguez et al. are based on a complete shape description; they exploit certain properties of the objects like symmetry and extrusion patterns [10], [11]. On the contrary to previous approaches, and trying to reduce the computational costs, Lei et al. have proposed to estimate a stable grasp using a force balance method instead of generating an accurate shape description [12]; this work is based on the usage of two depth images to establish the raw point cloud. Recently, Suzuki et al. have presented a system based on the previous approach, but by using a single depth image [7]. Their method is restricted to objects that not exceed the height of the gripper; moreover, their approach do not include any evaluation of the force applied with respect to the object physical properties.

A common way to define an stable grasp with finger gripers is through the evaluation of quality metrics based on force and form closure, which states the behavior of the object that was grasped across the laws of classical mechanics. Giacomo Mantriota proposed a criterion for the determination of optimal grip points to secure contact stability [13]. Other work have proposed and analyzed the uncertainty from so much the friction and contact position that focus in force-closure study [14]. There are few studies intended to grasping objects with passive gripper (vacuum gripper). In [15], the author has proposed to estimate the minimum value of the static friction coefficient and the vacuum level in order to guarantee a firm grasp of the object. Due to the previously mentioned research, a theoretical model was developed to determine the minimum value of the vacuum force able to guarantee a grasp and a criterion was proposed for the optimum gasping position [8].

III. Proposed Approach

The propose approach consists of two main stages: the first stage is related with the object's geometry extraction, based on 3D image processing algorithms (Sections III-A, III-B and III-C); the second stage is related with the estimation of the best grasping position, based on a force and moment balance formulation (Section III-D). These two stages are described next.

A. Data Acquisition and Segmentation

Initially, 3D data are acquired using a commercial camera. Three dimensional data contains information about the scene together with the objects to be grasped, hence the first step consists in segmenting the 3D data in order to keep only those points belonging to the objects of interest. The obtained raw cloud of point is processed in order to have only the objects of interest from it. Firstly, a simple depth filter is applied through the **X** and **Z** direction of the Camera Coordinate System (**CCS**) just to pick up points belonging to the robot workspace (all the points belonging to the base of the robot are removed). Figure 1 presents an illustration of the camera, robot and object coordinate systems. Secondly, the obtained cloud of points are down sampled using a voxel grid of fixed size with the aim of speeding up further processing. As illustrated in Fig. 1, the workspace consists of a table where objects are placed. Hence, in order to segment the objects and the table, a fitting process is applied to extract those points belonging to the table. The fitting process is based on a Random Sample Consensus (RANSAC) method, which iteratively finds the plane with the larger number of inliers. Outliers points corresponds to the objects present in the robot's workspace. Once the set of points corresponding to the objects are isolated, an Euclidean cluster segmentation is used to identify single objects, and to remove small set of points that does not belong to any objects. In summary, this first step results in a set of clusters of 3D points belonging to the different objects present in the robot's workspace.

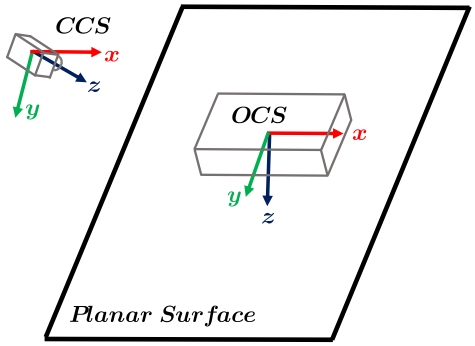

Fig. 1. Representation of the Camera Coordinate System **CCS** and Object Coordinate System **OCS**.

B. Object Pose Estimation

Once the cloud of points that represents the objects in the scene is obtained, their centroid and main orientations are estimated. The following process is applied to every object independently. Hence, for a given object (cloud of points), the best representation of it is needed in order to compute an accurate estimation of the minimum grasping force. The proposed approach assumes the object top surface is a plane, which is used as a reference to place the Object Coordinate System (**OCS**) (see Fig. 1); the object grasping will be performed through this plane. In this way, the centroid is determined using the concave surfaces of the two principal axis of the object, the first surface is obtained by the normal vector of the plane and the second surface is obtained by means of PCA. The centroid and main axis of orientation of the given object are determined by means of a two step Principal Component Analysis (PCA).

Firstly, the object points are projected to a plane in the ${}^{O}\mathbf{Z}$ direction[1]. Note the ${}^{O}\mathbf{Z}$ axis of the object coordinate system is placed so that it is normal to the plane fitted to the table of the workspace (see Section III-A). Then, the centroid of the concave hull of the projected cloud of points[2] is computed ${}^{C}G_1$. At the same time, the major ${}^{C}\mathbf{r}_1$ and minor ${}^{C}\mathbf{r}_2$ eigenvectors are estimated from the corresponding covariance matrix, these vectors are now considered as **X** and **Y** orientation axis respectively of the **OCS**.

Secondly, one of the two eigenvectors computed above (${}^{C}\mathbf{r}_1$, ${}^{C}\mathbf{r}_2$) is used as a reference for the next plane projection process. In order to do the eigenvector selection, the dot product between the viewing direction vector of the sensor (${}^{C}\mathbf{Z}$) and the estimated eigenvectors is computed; the eigenvector more parallel to the resultant vector (see eq. (1)) is selected as the normal vector (**n**) for the new plane projection:

$$\mathbf{n} = \begin{cases} {}^{C}\mathbf{r}_1, & \text{if } {}^{C}\mathbf{r}_1 \cdot {}^{C}\mathbf{Z} > {}^{C}\mathbf{r}_2 \cdot {}^{C}\mathbf{Z} \\ {}^{C}\mathbf{r}_2, & \text{if } {}^{C}\mathbf{r}_2 \cdot {}^{C}\mathbf{Z} \leq {}^{C}\mathbf{r}_1 \cdot {}^{C}\mathbf{Z} \end{cases} \tag{1}$$

The coefficients of the new plane model are determined from the implicit equation of the plane (eq. (2)) using the normal vector **n** and the centroid ${}^{C}G_1$ as follow:

$$ax + by + cz = d \tag{2}$$

where

$$a = n(x), b = n(y), c = n(z)$$
$$d = -[a({}^{C}G_1(x)) + b({}^{C}G_1(y)) + c({}^{C}G_1(z))]$$

Similarly to in the previous case, the original cloud of points corresponding to the given object is projected, but now onto the new plane model using the **n** direction; from that projection a new centroid (${}^{C}G_2$) is calculated by means of PCA; the final centroid ${}^{C}G_{Obj}$ takes into consideration the two representative perspectives of the object; in other words the 3D coordinates of ${}^{C}G_{Obj}$ are obtained from ${}^{C}G_1$ and ${}^{C}G_2$. Hence, the pose of the object coordinate system is defined as follows: the orientation is obtained as indicated in the first step; while the position corresponds to the centroid computed above ${}^{C}G_{Obj}$. This coordinate system is now referred from the camera coordinate system (**CCS**) to the Robot Coordinate System (**RCS**); this reference system update is just performed over the **OCS**, but not over the coordinates of the given cloud of points; in other words just the position and orientation of the **OCS** are referred to the robot coordinate system.

C. Mass Estimation

Although object's mass cannot be directly determined with just depth information, it can be estimated by assuming two additional considerations. Firstly, it is assumed that the density of the objects is uniform; secondly, it is assumed that the total volume of the object corresponds to the bounding envelope of it. Hence, the volume of the object is estimated to indirectly determine its mass. The volume measurement algorithm used in the current work is based on a modification of the approach presented in [16]. By using the object's centroid ${}^{C}G_{Obj}$, and eigenvectors ${}^{C}\mathbf{r}_1$ and ${}^{C}\mathbf{r}_2$ computed in the previous section, a Minimum-Volume Oriented Bounding Box (MVOBB) is obtained and fitted to the object. Then, in order to have a better estimation than just using the volume of a box, a filling rate value is considered. The filling rate value is obtained using a plane projection strategy similar to the method used to estimate the centroid in the previous section. The proposed strategy works as follows, initially a random number (K_T) of 3D points is selected; these points belong to the MVOBB computed above. Then, these points are projected onto the planes defined by the normal vectors (${}^{O}\mathbf{Z}$ and **n**), and the resulting points are evaluated to identify whether they match or not with the real object; the number of matched points (K_t) is used to compute the object properties (volume and mass) as follow:

$$Volume = (x_u - x_l)(y_u - y_l)(z_u - z_l)\frac{K_t}{K_T}$$

Consequently the mass of the object is obtained from:

$$Mass = \rho(x_u - x_l)(y_u - y_l)(z_u - z_l)\frac{K_t}{K_T} \tag{3}$$

where subindex u and l refers to the upper and lower limits of the **MVOBB** and ρ is a value that depends on the object's material.

D. Problem Formulation

This section tackles the estimation of the grasping position that requires the minimal vacuum force value, able to perform a reliable object grasping through a gripper with two suction cups. A reliable object grasping guarantees that the object will not slip or fall during the object manipulation. In order to compute to optimal position of the vacuum gripper on the top planar surface of the object, the criterion proposed in [8] is followed. The top planar surface of the object is used as an approximation to formulate the grasping problem in this section. In this section a new coordinate systems is introduced that will be referred to as the Surface Coordinate System (**SCS**). Figure 2 illustrates the top planar surface of a given object together with the reference system and suction cups. The **X** and **Y** axis of the reference system are contained in the top planar surface; similarly to previous works, the **SCS** is placed in the surface midpoint. According to [8] the best location for placing the vacuum gripper (i.e., minimal vacuum force) corresponds to the place of the surface coordinate system (**SCS**), but to avoid imposing additional constraints in the current work a general formulation is followed.

The forces applied by the suction cups are illustrated in Fig. 2; once the object comes into contact with the gripper, tangential forces are generated on the **X** and **Y** axes of each suction cup ($F_{t_{x1}}$,$F_{t_{y1}}$) and ($F_{t_{x2}}$,$F_{t_{y2}}$). Also each contact point generates a normal force to the contact surface ($F_{\mathbf{n}_1}$, $F_{\mathbf{n}_2}$), finally we have the force provided by the gripping device

[1]O refers to the object coordinate system (**OCS**)

[2]C refers to the camera coordinate system (**CCS**)

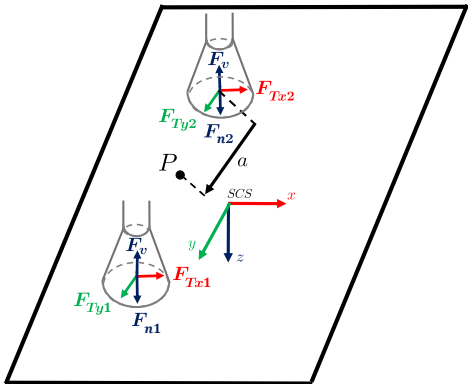

Fig. 2. Forces diagram when the suction cups stick on the surface, The midpoint between the suction cups is denoted by P.

($F_{\mathbf{v}}$). With all these vectors the force and torque balance is formulated looking for the minimum ($F_{\mathbf{v}}$).

The force balances in the three directions (**X**,**Y**,**Z**) of the **SCS** results in the following equations:

$$\begin{aligned} F_{e_x} + F_{t_{x1}} + F_{t_{x2}} &= 0 \\ F_{e_y} + F_{t_{y1}} + F_{t_{y2}} &= 0 \\ F_{e_z} - 2F_v + F_{n_1} + F_{n_2} &= 0 \end{aligned} \tag{4}$$

where $F_{\mathbf{e}}$ = (F_{e_x}, F_{e_y} and F_{e_z}) represents the external forces, which are related with the object weight and a rotation angle of the object with respect to a given axis; this rotation angle will be named as β. As mentioned in Section III-C, we assume that the object has equal density through all the geometry, hence, the object's mass can be easily estimated. After the force balances have been obtained, the moment balances in the three directions (X,Y,Z) of the **SCS** are formulated as follows:

$$\begin{aligned} T_{o_x} + T_{v_x} + T_{sc_{x1}} + T_{sc_{x2}} &= 0 \\ T_{o_y} + T_{v_y} + T_{sc_{y1}} + T_{sc_{y2}} &= 0 \\ T_{o_z} + T_{v_z} + T_{sc_{z1}} + T_{sc_{z2}} &= 0 \end{aligned} \tag{5}$$

where T_{o_x}, T_{o_y} and T_{o_z} are external torques that depend on the external forces and on the position of the objects centroid previously estimated (Section III-B). T_{v_x}, T_{v_y} and T_{v_z} are torques that depend on the external forces and on the location of the gripper (x_v,y_v). Finally ($T_{sc_{x1}}$,$T_{sc_{y1}}$,$T_{sc_{z1}}$) and ($T_{sc_{x2}}$,$T_{sc_{y2}}$,$T_{sc_{z2}}$) are torques that depend on the forces that are generated when the suction cups come in contact with the object and on the distance defined between the center of each suction cup and the **SCS**.

According to [17] a positive constraint is that the normal force component must be positive for guaranteeing a grasp and preventing that object from falling; in other words $F_{\mathbf{n}_i} > 0$, for i = {1, 2}. As mentioned before, the friction constraint tell us the tangential force components of each contact point; it must satisfy the following limitation, in order the suction cup do not slip when there is contact with the object [17]:

$$\sqrt{F_{t_{xi}}^2 + F_{t_{yi}}^2} = \mu F_{\mathbf{n}_i}$$

The no-lineal equations resulting from the friction constraints are quite difficult to solve. In [17] a linear form of this constraint is proposed; where a geometrical relation is obtained considering an imaginary friction pyramid inscribed within the friction cone. Due the geometrical relation, the new friction constraint can be expressed as two linear relations:

$$\begin{aligned} -\mu\frac{F_{\mathbf{n}_i}}{\sqrt{2}} \leq F_{t_{xi}} \leq \mu\frac{F_{\mathbf{n}_i}}{\sqrt{2}} \\ -\mu\frac{F_{\mathbf{n}_i}}{\sqrt{2}} \leq F_{t_{yi}} \leq \mu\frac{F_{\mathbf{n}_i}}{\sqrt{2}} \end{aligned}$$

These relations split up into four inequalities:

$$\begin{aligned} -F_{t_{xi}} - \mu\frac{F_{\mathbf{n}_i}}{\sqrt{2}} \leq 0 \\ F_{t_{xi}} - \mu\frac{F_{\mathbf{n}_i}}{\sqrt{2}} \leq 0 \\ -F_{t_{yi}} - \mu\frac{F_{\mathbf{n}_i}}{\sqrt{2}} \leq 0 \\ F_{t_{yi}} - \mu\frac{F_{\mathbf{n}_i}}{\sqrt{2}} \leq 0 \end{aligned} \tag{6}$$

Finally, with all the above formulations (force balance, moment balance and friction constraint) the following equation systems are obtained:

$$\begin{aligned} F_{e_x} + F_{t_{x1}} + F_{t_{x2}} &= 0 \\ F_{e_y} + F_{t_{y1}} + F_{t_{y2}} &= 0 \\ F_{e_x} - 2F_v + F_{\mathbf{n}1} + F_{\mathbf{n}2} &= 0 \\ T_{o_x} + T_{v_x} + T_{sc_x1} + T_{sc_x2} &= 0 \\ T_{o_y} + T_{v_y} + T_{sc_y1} + T_{sc_y2} &= 0 \\ T_{o_z} + T_{v_z} + T_{sc_z1} + T_{sc_z2} &= 0 \\ F_{\mathbf{n}_i} > 0; \qquad i &= 1,2 \\ -F_{t_{xi}} - \mu\frac{F_{\mathbf{n}_i}}{\sqrt{2}} \leq 0; \qquad i &= 1,2 \\ +F_{t_{xi}} - \mu\frac{F_{\mathbf{n}_i}}{\sqrt{2}} \leq 0; \qquad i &= 1,2 \\ -F_{t_{yi}} - \mu\frac{F_{\mathbf{n}_i}}{\sqrt{2}} \leq 0; \qquad i &= 1,2 \\ +F_{t_{yi}} - \mu\frac{F_{\mathbf{n}_i}}{\sqrt{2}} \leq 0; \qquad i &= 1,2 \end{aligned} \tag{7}$$

The solution of the equation systems previously defined allows us to find the minimal vacuum force ($F_{v_{min}}$) necessary to avoid falling or slipping when the object is manipulated.

IV. Experiments

The proposed approach is evaluated with a set of experiments in a real scenario using several objects with different sizes and geometries. The first set of experiments focuses in measuring the accuracy with which the vision system determines the position where the gripper should be placed. The second set of experiments test the performance of grasping in terms of the holding stability of the objects, these experiments consider two aspects: the vacuum force and the applied

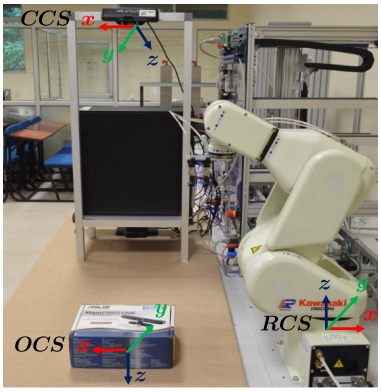

Fig. 3. Illustration of the working space, camera coordinate systems corresponding to the robot, camera and object are indicated.

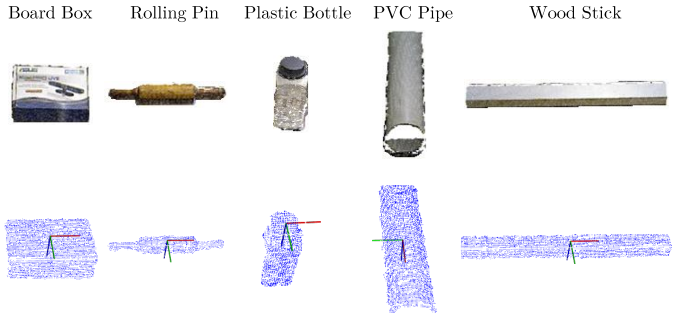

Fig. 4. Objects used for evaluating the proposed approach. At the top row the point cloud representations of the given objects, taken from a single view, are depicted. At the bottom row, the resulting point cloud and the definition of the Surface Coordinate System (SCS) are presented.

rotation (β angle mentioned in Section III-D, which measures the difference in orientation between the original position and the final one).

A. Experimental Setup

All the experiments are conducted using a 6 DOF robotic arm with a two suction cups vacuum gripper, which has three defined values of vacuum forces. The vision system configuration consists of an Asus Xtion Pro sensor (640×480 pixels at 30fps) and a HP Compact Pro 6300 PC (Intel ® Core ™ CPU i7-3770 @3.40 GHz, 8GB RAM). Data acquisition and processing are implemented in C++ using the Point Cloud Library (PCL) [18]. Figure 3 shows an illustration of the robot workspace and setup.

B. Position Accuracy

In this section the grasping position that return the vision system is compared with the real position based on the consideration of force balance studied in Section III-D. The test also consider the rotation of the object with respect to the view perspective of the sensor.

The group of objects and the visual results are presented in the Fig. 4, and the different position errors are shown in the Table I. It can be seen that in comparison to the other objects the *PVC pipe* has a relatively higher error value. That is because the aforementioned object has a internal hollow volume. The missing information makes difficult to represent the shape of the front part of the object for which the centroid with respect the **Z** coordinate of the (**SCS**) is calculated; in fact the **Z** component is actually the one that is incorrectly estimated. On the other hand, the rest of objects have an error lower than 5.3mm in all the components regardless of whether they have different shapes. In addition, the object rotation increased slightly the error in the Y coordinate and decreased in the X coordinate, so the perspective takes an important factor to the system.

C. Grasping Performance

This section assesses the grasp of the object according to the applied vacuum force when the grasp device is placed in the **SCS** (optimal position). It should be pointed out that in Section III-C, it is assumed that the object to be picked has a solid volume, then the mass estimation is not suitable when quotidian objects (*board box*, *PVC pipe*) with hollow volume are considered.

TABLE I
POSITION ERROR

Object	Rotation	Error (mm)		
		X	Y	Z
Board Box	0°	3.5	2.4	1.3
	45°	1.9	4.8	2.4
Rolling Pin	0°	4.2	1.1	2.2
	45°	3.3	3.6	1.8
PVC Pipe	0°	7.2	1.8	20.6
	45°	10.2	10.4	20.5
Wood Stick	0°	4.1	1.1	1.9
	30°	3.8	1.9	1.1
Plastic Bottle	0°	5.3	2.2	2.1

Vacuum force, vacuum level, and the grasp results are depicted in Table II. The minimal force required for the grasp of *board box* and *PVC pipe* is in the range I and II respectively. If these objects were solid, then the vacuum force would be greater. Heavy objects such as *wood stick* and *full plastic bottle*, require a minimum vacuum force that is in range 3. In comparison to other objects the *rolling pin* has the best grasp result due to this object has a uniform density, the minimal force in this case is located in the range I.

In Table III, it is shown how the position of vacuum gripper affects the vacuum force (an illustration is provided in Fig. 5). The *rolling pin* object is considered as a case study in this experiment. It is verified that the optimum position to generate a minimal force is when the mid point between suction cups coincides with the **SCS** (see Fig. 4), that is, in this position it requires 2.67 N to grasp the object; however for Xv = 4 cm and Yv = 0 cm a notable increase of the vacuum force is required, going from 2.67 N to 8.13 N. An additional test is performed in this case study by locating the gripper in the optimal position but rotating the object with a β = 30° respect to the **X** axis of **SCS**, the grasping performance was evaluated for three vacuum level:

TABLE II
GRASPING RESULTS FOR EACH OBJECT WHEN THE LOCATION OF GRIPPER COINCIDE WITH THE SCS

Range	Vacuum Force (N)	Vacuum Pressure (bar)	Board box	Rolling pin	PVC pipe	Plastic Bottle	Wood stick
I	2 - 4	0.6	OK	OK	Fail	Fail	Fail
II	6 - 8	0.8	OK	OK	OK	Fail	Fail
III	9 - 11	1.4	OK	OK	OK	OK	OK

TABLE III
GRASPING EVALUATION FOR THE *rolling pin* (**1ST ROW**: OPTIMAL GRASPING COMPUTED WITH THE PROPOSED APPROACH)

Position (cm)	β	0.6 (bar)	0.8 (bar)	1.4 (bar)
0.0	0°	OK	OK	OK
4.0	0°	Fail	Fail	OK
0.0	30°	Fail	Fail	OK

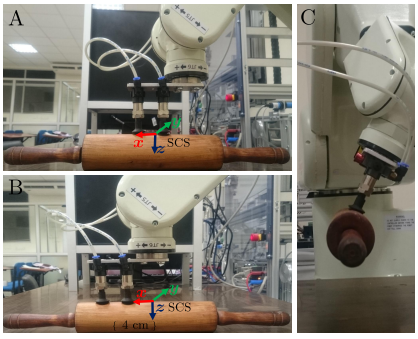

Fig. 5. Case study: (A) the mid point between suction cups coincide with the **SCS**; (B): the vacuum gripper moves 4 cm in the **X** direction; (C): the angle of rotation is 30°, the object does not fall with a pressure of 1.4 bar.

- 0.6 (bar): fails to grasp the object.
- 0.8 (bar): object fell for $\beta = 23°$.
- 1.4 (bar): object was successfully grasped.

V. CONCLUSION

This paper presents a novel approach for optimal grasp vacuum grippers estimation based on the usage of a 3D vision system. Although only three different vacuum forces have been considered, experiments show the validity of the proposed approach. As future work several possibilities will be explored. Firstly, on the object geometry extraction side, multi-view approaches will be explored in order to have a more precise 3D object information; regarding the object representation the usage of 3D mesh will be explored to fit the objects, instead of **MVOBB**. Another possible improvement will be to incorporate an additional sensor to estimate the material properties, in the sense that a wide variety of objects with less restrictions can be considered. Finally, regarding the grasp mathematical model, a more general model will be studied in order to avoid the top planar surface assumption.

ACKNOWLEDGMENTS

This work has been partially supported by the following projects: ESPOL-M1-DI-2015; ESPOL-G4-DI-2014; and TIN2014-56919-C3-2-R (Spanish Government).

REFERENCES

[1] V. Lippiello, "Grasp the possibilities: Anthropomorphic grasp synthesis based on the object dynamic properties," *IEEE Robotics & Automation Magazine*, vol. 22, no. 4, pp. 69–79, 2015.

[2] M. Ribo and M. Brandner, "State of the art on vision-based structured light systems for 3d measurements," in *Robotic Sensors: Robotic and Sensor Environments, 2005. International Workshop on*. IEEE, 2005, pp. 2–6.

[3] E. N. Malamas, E. G. Petrakis, M. Zervakis, L. Petit, and J.-D. Legat, "A survey on industrial vision systems, applications and tools," *Image and vision computing*, vol. 21, no. 2, pp. 171–188, 2003.

[4] J.-K. Oh and C.-H. Lee, "Development of a stereo vision system for industrial robots," in *Control, Automation and Systems, 2007. ICCAS'07. International Conference on*. IEEE, 2007, pp. 659–663.

[5] G. Ros, A. Sappa, D. Ponsa, and A. M. Lopez, "Visual slam for driverless cars: A brief survey," in *Intelligent Vehicles Symposium (IV) Workshops*, vol. 2, 2012.

[6] D. Gerónimo, A. López, and A. D. Sappa, "Computer vision approaches to pedestrian detection: visible spectrum survey," in *Iberian Conference on Pattern Recognition and Image Analysis*. Springer, 2007, pp. 547–554.

[7] T. Suzuki and T. Oka, "Grasping of unknown objects on a planar surface using a single depth image," in *Advanced Intelligent Mechatronics (AIM), 2016 IEEE International Conference on*. IEEE, 2016, pp. 572–577.

[8] G. Mantriota, "Optimal grasp of vacuum grippers with multiple suction cups," *Mechanism and machine theory*, vol. 42, no. 1, pp. 18–33, 2007.

[9] L. F. Gallardo and V. Kyrki, "Detection of parametrized 3-d primitives from stereo for robotic grasping," in *Advanced Robotics (ICAR), 2011 15th International Conference on*. IEEE, 2011, pp. 55–60.

[10] A. H. Quispe, B. Milville, M. A. Gutiérrez, C. Erdogan, M. Stilman, H. Christensen, and H. B. Amor, "Exploiting symmetries and extrusions for grasping household objects," in *Robotics and Automation (ICRA), 2015 IEEE International Conference on*. IEEE, 2015, pp. 3702–3708.

[11] J. Bohg, M. Johnson-Roberson, B. León, J. Felip, X. Gratal, N. Bergström, D. Kragic, and A. Morales, "Mind the gap-robotic grasping under incomplete observation," in *Robotics and Automation (ICRA), 2011 IEEE International Conference on*. IEEE, 2011, pp. 686–693.

[12] Q. Lei and M. Wisse, "Fast grasping of unknown objects using force balance optimization," in *Intelligent Robots and Systems (IROS 2014), 2014 IEEE/RSJ International Conference on*. IEEE, 2014, pp. 2454–2460.

[13] G. Mantriota, "Communication on optimal grip points for contact stability," *The International Journal of Robotics Research*, vol. 18, no. 5, pp. 502–513, 1999.

[14] Y. Zheng and W.-H. Qian, "Coping with the grasping uncertainties in force-closure analysis," *The International Journal of Robotics Research*, vol. 24, no. 4, pp. 311–327, 2005.

[15] G. Mantriota, "Theoretical model of the grasp with vacuum gripper," *Mechanism and machine theory*, vol. 42, no. 1, pp. 2–17, 2007.

[16] J. Siswantoro, A. S. Prabuwono, and A. Abdullah, "Volume measurement algorithm for food product with irregular shape using computer vision based on monte carlo method," *Journal of ICT Research and Applications*, vol. 8, no. 1, pp. 1–17, 2014.

[17] K. B. Shimoga, "Robot grasp synthesis algorithms: A survey," *The International Journal of Robotics Research*, vol. 15, no. 3, pp. 230–266, 1996.

[18] R. B. Rusu and S. Cousins, "3d is here: Point cloud library (pcl)," in *Robotics and Automation (ICRA), 2011 IEEE International Conference on*. IEEE, 2011, pp. 1–4.